Space Debris Removal Using Swarm Technology

Winnie Tang *
Thales, Above Water Systems, Sydney, Australia.
winnie.tang2@unswalumni.com

The growing accumulation of space debris in Low Earth Orbit (LEO) threatens the safety and sustainability of space operations. This study proposes a swarm-based Active Debris Removal (ADR) mission, utilizing autonomous CubeSat swarm agents, named SwarmSats, to rendezvous, capture, and aggregate debris, enhancing their Radar Cross-Section (RCS) and decay rate. To validate feasibility, debris targets were selected based on size, shape, weight, and inclination. Simulations in STK, TAROT, and Jupyter Notebook Python (Pygame & Matplotlib 3D) modeled orbital interactions, access windows, and swarm dynamics. SwarmSats were tested for collision avoidance, optimal path planning, fuel efficiency, and debris stabilization. Additional calculations assessed Ultra-High Molecular Weight Polyethylene (UHMWPE) nets and electromagnetic coils for debris aggregation and deorbiting.

Findings confirm the viability of multi-agent swarm robotics for large-scale debris mitigation. Future work will refine optimization algorithms, real-time decision-making, and advanced stabilization strategies, forming a foundation for next-generation ADR missions.
Keywords: space debris, LEO, space, mission concept, multi-agent systems, swarm robotics

Nomenclature

A	Area through which heat is being transferred, (m^2)
F	Force, (N)
F	Thrust, (N)
G	Gravitational constant, 6.643×10^{-11} (Nm^2/kg^2)
M	Mass of earth = 5.972×10^{24} (kg)
Q	Heat transfer rate, (Watts)
ΔT	The temperature difference across the material, (°C)
ΔV	Total change in velocity, (m/s)
a	Acceleration (m/s^2)
Δi	Change in inclination measured in degrees
Δp	Change in momentum, (km/s)
Δv	Change in velocity, (m/s)
I	Moment of inertia, ($kg.m^2$)
k	Thermal conductivity of the material, (W/m·K)
m	Mass of debris, (kg)
ω	Angular velocity, (rad/s)
r	Radius
r	Semi-major axis, (km)
v	Relative velocity, (m/s)

*Self-funded research based on undergraduate honours thesis in the University of New South Wales (UNSW), School of Mechanical Manufacturing.

Acronyms & Abbreviations

ADR Active Debris Removal
COM Center of Mass
RCS Radar Cross-Section
STK Systems Tools Kit [1]
TAROT Terrestrial and Astronomical Rapid Observation Toolkit [2]
TLE Two-Line Element
UHMWPE Ultra-High Molecular Weight Polyethylene

I. Introduction

The increasing density of space debris in Low Earth Orbit (LEO) poses a significant and growing risk to active satellites, space missions, and human spaceflight. Defunct satellites, spent rocket stages, and disintegrated spacecraft travel at high velocities across various orbital altitudes, creating a persistent collision hazard for operational spacecraft [3]. Even the smallest fragment of orbital debris can cause catastrophic damage—acting like a bullet at orbital speeds. Notably, the ISS cupola window currently bears a visible chip caused by a millimetre-sized debris particle, highlighting the constant risk faced by astronauts during extravehicular activities (EVAs) [4]. In the event of a collision, debris fragments multiply, initiating a cascading effect known as the Kessler Syndrome, further exacerbating the hazard to space operations [5].

To ensure the long-term viability of space activities, a mission concept using swarm robotics, is proposed as an effective and sustainable method of capture and removal of debris. This explores the feasibility of deploying swarm agent CubeSats, named SwarmSats, as part of a multi-agent system to autonomously capture and stabilize debris using a combination of nets, electromagnetic adhesion, and controlled maneuver as a scalable solution. The methodology in this paper aligns with a systems engineering approach to optimize the feasibility of swarm-based ADR. This structure follows the mission planning approach for space debris removal by minimizing fuel consumption through a structured multi-stage process recommended by Cerf [6]. The proposed research extends the concept of single-agent mission planning with high-thrust and low-thrust vehicles, by leveraging swarm robotics, where multiple autonomous agents collectively perform debris capture and stabilization. While most ADR concepts refine mission trajectories post-optimization, the proposed swarm approach uses adaptive control algorithms to dynamically adjust agent positioning and capture strategies based on real-time debris motion.

This paper is built on the existing groundwork and simulations developed in Tang's Honours thesis [7]. Terrestrial and Astronomical Rapid Observation Toolkit (TAROT) and Systems Tools Kit (STK) were the programs utilized for identification of optimal debris targets based on orbital characteristics. A novel Python-based simulation framework was developed to model agent behavior, collision avoidance, and swarm dynamics for effective debris retrieval. The analysis assesses mission feasibility by evaluating fuel consumption, net material selection, and the ability to stabilize tumbling debris to further validate the concept. The mission concept proposal for this feasibility study is shown in Figure 1, depicting a five-stage process for removing space debris using a multi-agent system approach.

1. First stage: Mothership Launch

The debris removal mission begins with the launch of a mothership on a rocket such as a Delta IV or ATLAS, which is capable of carrying small payloads and refueling into the highest level of LEO. This mothership contains the SwarmSats that will perform the debris removal tasks. It is designed to lower its altitude gradually without station keeping, facilitating the deployment of SwarmSats and allowing for their potential return to the mothership for refueling. Once the mothership reaches the designated orbital region, small SwarmSats, comparable in size and design to the RemoveDebris [8] CubeSat, are deployed.

2. Second Stage: SwarmSat Deployment

Each SwarmSat is equipped with machine learning algorithms to navigate the dynamic space environment and have the space debris catalog stored on board. The agents are equipped with a net-like material made of Ultra-High-Molecular-Weight Polyethylene (UHMWPE), chosen for its flexibility, durability, and cost viability. Upon deployment, the agents seek out the target debris pieces or clusters, capturing them with the net. These clumps of debris will then be connected to create a 'debris chain', to increase their size and weight to assist with deorbiting. These SwarmSats have radar sensors and onboard path optimization. They are responsible for storing information on space debris and maintaining a communication link with ground control for updates and commands.

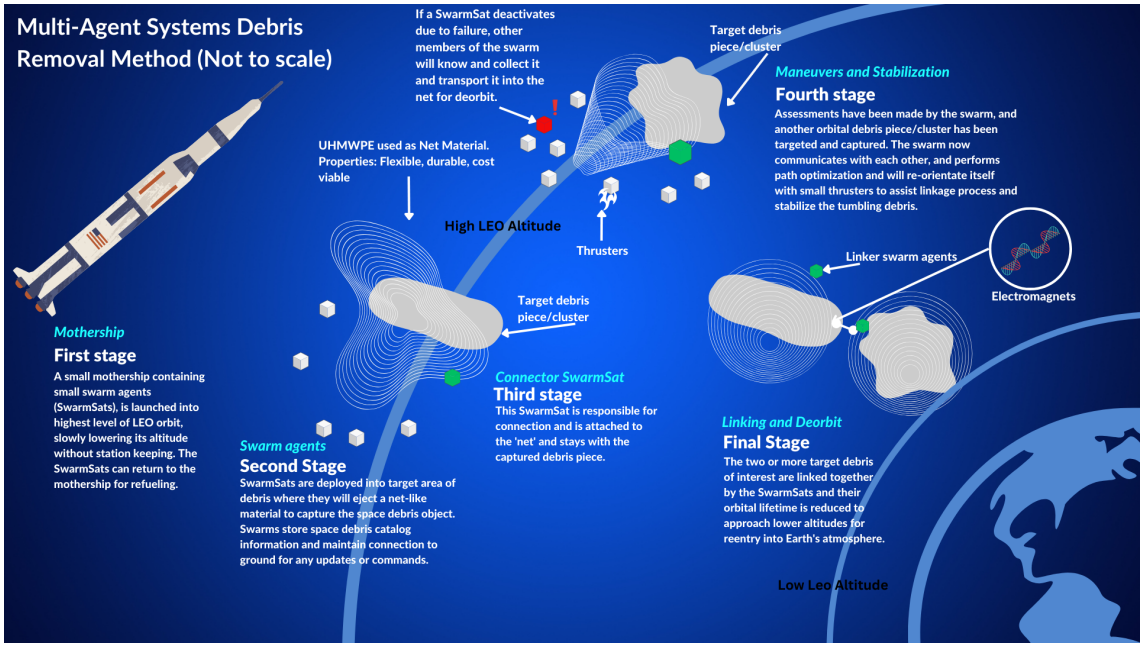

Fig. 1 Mission Concept Proposal [7]

3. Third Stage: Connector SwarmSat Engagement

In this stage, specialized connector SwarmSats, are deployed for linking. They are tasked with securing the captured debris within the net. These connector agents are responsible for maintaining the captured debris, ensuring that the tethering process is successful and that the debris remains contained.

4. Fourth Stage: Maneuvers and stabilization

After a piece of debris or a cluster of targets has been captured, SwarmSats conduct evaluations to locate additional debris. The SwarmSats communicate with each other optimizing the path for debris collection. Fuel is consumed as the SwarmSats try to stabilize the tumbling debris during capture and to match the ΔV between the two pieces of debris.

5. Final Stage: Linking and Deorbit

The culmination of the process involves linking two or more pieces of target debris together. There are electromagnets that have determined position points of contacts on the UHMWPE net; these electromagnets are activated to bring the captured debris pieces closer together for connection. They are equipped with small thrusters that assist in the reorientation of both the SwarmSats and the tumbling debris, ensuring proper linkage and stabilization for the removal process. By mechanically connecting the debris, the combined object has a larger cross-sectional area, which increases drag and consequently reduces the orbital lifetime. This linked debris is then guided by the SwarmSats to lower altitudes, where atmospheric drag is sufficient to naturally deorbit the debris and ensure its re-entry and disintegration in Earth's atmosphere.

II. Methods

To systematically prove the feasibility of the proposed mission concept, the study was divided into several key components—debris selection and mission feasibility simulations, and theory and calculations for mission considerations. This structured breakdown ensures that each aspect of the mission is evaluated in depth while maintaining traceability between concept development and technical validation.

A. Debris Selection and Mission Feasibility Simulations

The mission is defined by the parameters provided by NASA, which has identified the top risk space debris to be those that are 3mm and smaller size existing in the 600 to 1000km altitude in LEO [9]. They are too small to be consistently tracked by current radar systems but can still puncture spacecraft at orbital velocities. Peterson et. al [10] emphasizes that the concern are the break up of large intact objects (i.e. rocket bodies and satellites) that have

high mass and kinetic energy, posing the greatest threat of generating huge amounts of small, hazardous debris in the future if they collide. Colvin et. al [11] indicates that the most effective remediation methods to reduce risks to operators are approaches for removing small debris and nudging larger debris to avoid collisions.

The focus of this research hence targets space debris objects of small Radar Cross-Section (RCS) as part of the mission definition phase. This phase establishes mission requirements-target selection criteria (inclination, altitude, accessibility). Space debris objects are cataloged in the European Space Agency (ESA) database, with the exception that there are some unidentified pieces in orbit. This catalog is reviewed and certain pieces are selected for analysis and simulation as part of the project.

Six pieces of debris were selected for analysis: four from Fengyun 1-C and two from CZ-6A. Fengyun-1C, was a Chinese weather satellite that was intentionally destroyed in 2007 for anti-satellite missile testing, creating over 3000 trackable debris fragments of different sizes [12]. Four pieces of the broken satellite Fengyun-1C (NORAD CAT ID: 31228, 31336, 32130 and 31627) were selected. Two pieces of CZ-6A (NORAD CAT ID: 54974 and 56629), originally part of a Chinese rocket body, were also selected because of their similar inclinations and orbital periods. The relative movement is tracked against other objects in the locked orbit on TAROT and their velocities were recorded. Their properties were retrieved from SpaceTrack [13]. TAROT [2] was only used to visualize the movement of debris objects in real time, where available data on the object's speed, inclination, altitude, and relative movement around other debris pieces were analyzed. This provided an additional validation method by allowing direct comparison of predicted motion paths with real observational data, helping refine trajectory predictions and agent maneuvering strategies. The data collected from the SpaceTrack is shown in Figure 2 and Table 1 below.

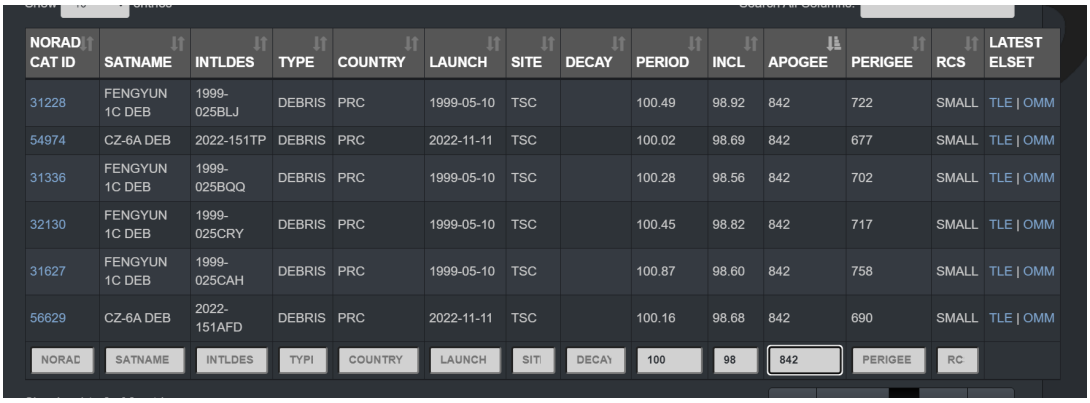

Fig. 2 6 pieces of selected debris in similar inclinations obtained from Spacetrack.org [13]

Table 1 Fengyun-1C and CZ-6A NORAD CAT ID's Comparative Data

Norad CAT ID	31228	31336	32130	31627	54974	56629
Period	100.49 min	100.28 min	100.45 min	100.87 min	100.2 min	100.16 min
Inclination	98°92′	98°56′	98°82′	98°60′	98°69′	98°68′
Velocity	7.4 km/s	7.4 km/s	7.4 km/s	7.5 km/s	7.6 km/s	7.5 km/s
Altitude	731.1 km	708.6 km	776.2 km	758.4	670.4 km	688.4 km
Apogee	842 km	842 km	842 km	842 km	842 km	842 km
Perigee	722 km	702 km	717 km	758 km	677km	690 km

Figure 3 shows the selected Fengyun-1A and CZ-6A debris objects modelled at a specific time frame. In this case, the 1st January 2024 was the selected date. TAROT shows the six debris pieces moving relative to each other in their specified orbits. The real time data of the six pieces of debris shows that the velocities are oscillating at a ±0.1 km/s, although this is a minor uncertainty, it indicates that the SwarmSats must take into consideration the velocity difference as it tries to capture, connect and stabilize these pieces of debris. The program can also filter out or include other objects. This is useful to visualize the selected debris objects against other objects in space. In the Figure 4, Fengyun-1C and CZ-6A are modelled against other space debris objects. This allows users to visualize nearby space debris objects to the selected objects. In this selected time interval, it can be observed that the six pieces are quite scattered, indicating the SwarmSats would not be linking the pieces simultaneously but capturing other objects nearby instead.

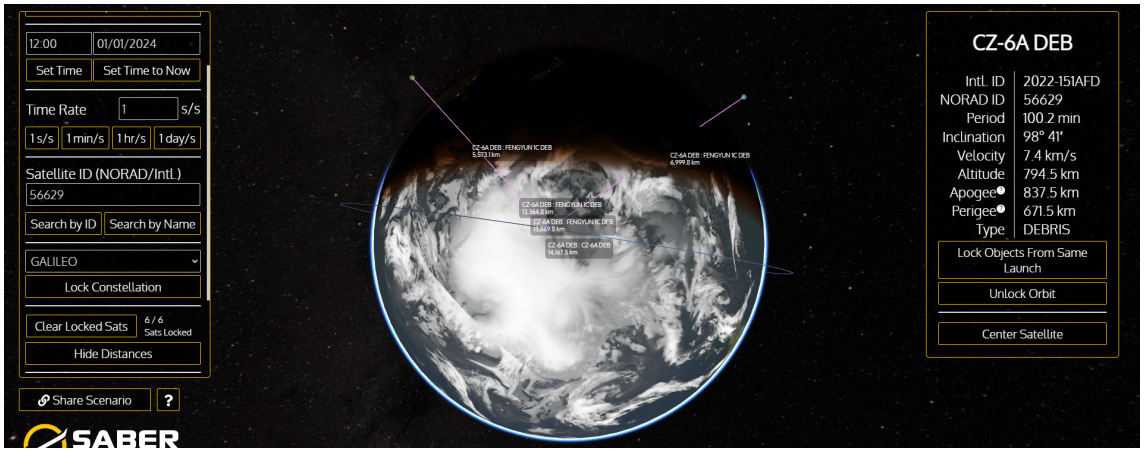

Fig. 3 Fengyun-1C and CZ-6A selected pieces modelled on TAROT[2].

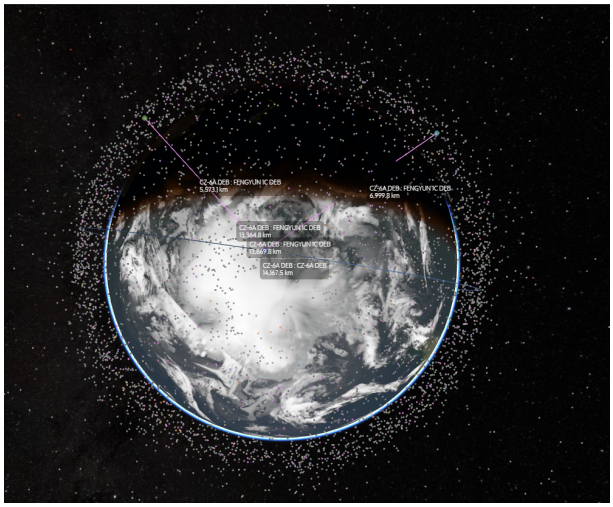

Fig. 4 Fengyun-1C and CZ-6A selected pieces relative to other debris modeled on TAROT[2].

SwarmSats use nets to capture and link two or more pieces of debris together to increase their cross-section and weight. After data collection and analysis of appropriate debris pieces, mathematical concepts must be implemented to verify the feasibility of the mission.

A mathematical framework was established based on Wertz et al.'s Space Mission Analysis and Design [14] combined with the concepts explored in Curtis's Orbital Mechanics for Engineering Students [15]. These calculations will determine the required change in velocity, Δv, for a SwarmSat to get from one debris piece to another. The swarm simulations also followed these mathematical principles*.

The following conditions below were made for this mission concept scenario between two debris pieces for a more feasible rendezvous. Appropriate parameters were established based on literature and the capabilities of an average CubeSat provided by NanoAvionics [16]. It is thus determined that for a feasible rendezvous:

- Inclination difference should be around ±0.5° to 1°
- The altitude difference should be no more than ±50 km from the target's altitude.
- Apogee and perigee values should be close to it's target, around ±20 km. The space debris objects should ideally have the same eccentricity.

Table 2 presents the access durations between the swarm agent (SwarmSat1) and each selected debris object, as simulated in STK over a one-month interval from 1 January to 1 February 2024. The term "access" refers to the periods when line-of-sight visibility exists between SwarmSat1 and the debris object, meaning they are within range for potential observation, communication, or rendezvous maneuver planning.

*These calculations are elaborated in Tang's Honours thesis [7] and can be provided upon request.

Table 2 SwarmSat1 access and contact to Fengyun-1C and CZ-6A debris pieces

Norad CAT ID	31228	31336	32130	31627	54974	56629
Min Duration (s)	888	176.009	177.924	N/A	22.352	3
Max Duration (s)	987.250	415784.476	314265.376	N/A	370	107
Min Duration Date	1 Feb 2024	7 Jan 2024	13 Jan 2024	N/A	15 Jan 2024	11 Jan 2024
Max Duration Date	15 Feb 2024	9 Jan 2024	15 Jan 2024	N/A	31 Jan 2024	15 Jan 2024
Mean Duration (s)	952.19	5801.363	4137.244	N/A	1600.01	1089.960
Total Duration (s)	845544.628	585937.696	533704.462	N/A	465140.28	319358.219

These durations represent windows of opportunity when SwarmSat1 can theoretically establish contact or begin an approach toward each debris target. The results help determine how frequently and for how long SwarmSat1 could engage each debris object, guiding optimal timing for capture and linking. As demonstrated with the selected pair CZ-6A DEB 54974 and 56629, access data—combined with orbital parameters—feeds into ΔV and rendezvous calculations to validate the feasibility of the swarm mission concept. Two pieces of debris were selected to substitute into the mathematical formulas. Based off Table 1, CZ-6A (NORAD CAT ID: 54974 and 56629) have the closest inclinations upon observation and thus would indicate a reduced fuel consumption. These calculations are reflected in Appendix A. A Δv of 3.41 m/s is quite low in the context of space missions, and is quite feasible and fuel-efficient for the SwarmSats. This value represents a very small velocity change required to transfer between the initial orbit r_1 and the target orbit r_2 using a Hohmann transfer. The difference between the orbital period is only 0.3 mins, which indicates that the orbits are only of slightly different energies. Both pieces of debris are traveling at an average speed of 7.5 km/s which simplifies the rendezvous. The altitudes are close and hence the ΔV is very small. This is because they have similar inclinations and velocities, hence the rendezvous process would be successful theoretically. These calculations should be applied to all the selected debris and SwarmSats. By aligning these calculations with access reports [†], an optimal time frame for capture could be determined.

1. 2D Simulations in Python

A simulation[‡] of the SwarmSats was conducted using Python in the Pygame library. The simulation is implemented in a local Cartesian inertial frame, where agent motion is simplified to basic vector updates with collision avoidance and basic pursuit logic. Detailed simulations with orbital motion are extremely complex and depend on specific mission requirements. The primary objective of the simulation was to assess swarm convergence, formation control, and collision avoidance when maneuvering towards a designated debris target within a certain orbital radius to support proof-of-concept.

Ten SwarmSats were selected as part of the simulation and each SwarmSat is represented as a sphere or 'particle', building on the work of Simone et. al [17]. The size of the workspace (not to scale) and the number of agents is defined as part of the simulation environment. The agent class is then defined to represent the properties and behaviors of individual agents. In this simplified simulation, the agents are considered to be in random co-ordinates in space and are assigned random position and velocity vectors to represent a realistic scenario where agents are scattered. These agents can then be attracted or repelled from certain points or other agents. Collision avoidance has been implemented in the simulation as an extension of Tang's Honours thesis [7], which has been suggested by Lupu [§] after a review.

The agents move at a uniform speed towards the formation radius in which the Center of Mass (COM) is located. In each iteration of the simulation loop, the COM of the swarm is calculated by averaging the positions of all agents. The COM represents the hypothetical center of the entire swarm, and can also be classified as the target in this scenario. Each agent updates its position based on its initial position and velocity. The agent's velocity is adjusted to steer it towards the COM. Over time, the agents move closer to the COM and start clustering together until they converge to a point at or near the COM. Collision avoidance algorithm implementation prevents agent overlap and ensures optimal trajectory adjustments. This feature represents proximity-based repulsion and enables agents to self-organize within a predefined formation radius for configuration stability and minimal fuel expenditure. Figure 5 shows the screenshots of different phases in the simulation. The circle demonstrates how swarm behaviour can be used to maintain a specific formation or spatial arrangement. The agents adjust their positions and velocities to avoid moving too far from each other and to stay within the defined formation radius. In a practical application, this circle could represent a desired formation or configuration that the swarm needs to maintain around a central

[†]These access reports generated in STK can be provided upon request.

[‡]Code available upon request.

[§]Sorina Lupu. Researcher at Caltech.

point of interest, such as a piece of space debris. The simulation demonstrates how swarm behavior can be used to achieve collective goals, such as convergence or clustering.

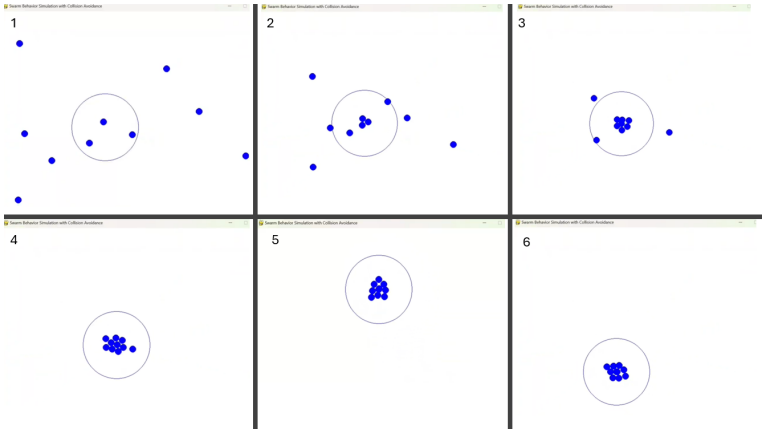

Fig. 5 Swarm Collision Avoidance Simulation

Dynamic debris movement and real-time stabilization mechanics were then implemented into the model. The screenshots of a run of this simulation is shown in Figure 6 below. The code is written so that it evaluates agent coordination strategies for stabilizing erratic motion, critical to mission success for ADR. Similarly, ten SwarmSats, labeled from 1-10, were assigned initial random positions and velocities, simulating scatter in real-life deployment scenarios. The debris object is then simulated to move in an unpredictable path, in a circular tumbling motion. Agents first track the tumbling debris and attempt to synchronize their movement, and within the capture range (yellow circle indicating the desired radius), the first agent secures the debris which is represented by the debris turning from red to green. Three agents were estimated to stabilize the debris, reducing motion within a stabilization radius of 100 pixels. The simulation output debris data for this run is available in Appendix B. Each time the simulation is run, the agents and debris generate in random coordinates thus providing different code outputs.

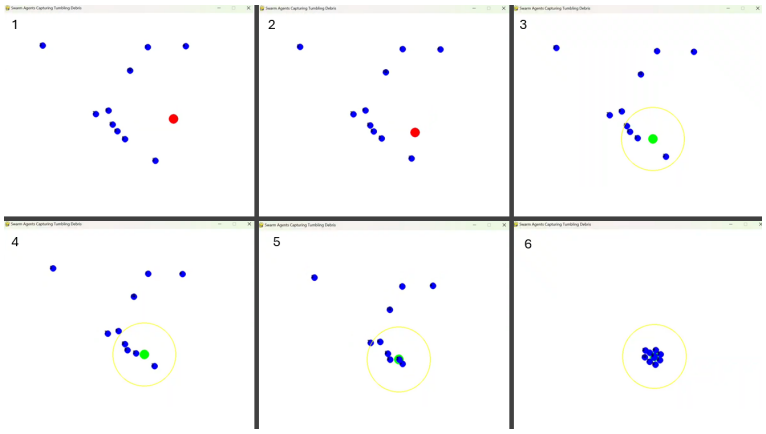

Fig. 6 SwarmSats Capturing Tumbling Debris

2. 3D Simulations in Python

To bridge the gap between conceptual validation and real-world application, a 3D simulation was developed using Matplotlib in a 3D space representation. Similarly to the 2D simulations, agents were deployed randomly in a 3D environment, with the exception of introducing an additional z-axis component. The debris followed a tumbling motion in all three dimensions, hence making capture more complex and requiring enhanced tracking behavior. Collision avoidance was extended to three axes, ensuring spatial awareness among agents. Capture and stabilization remained consistent with the 2D model, requiring at least 3 agents to stabilize the debris, but now requiring optimized approach angles due to the additional degree of freedom. Figure 7 shows the visual output of the 3D simulation, the results from the code are shown in Appendix C.

Whilst the 2D model showed fundamental swarm behavior, this 3D model proves feasibility in an orbital context. By showing that SwarmSats can still capture and stabilize debris in 3D space, the viability of multi-agent ADR

operations is further validated. Different runs of the simulation are reflected in Appendix D and Appendix E. The code for all these simulations can be provided upon request.

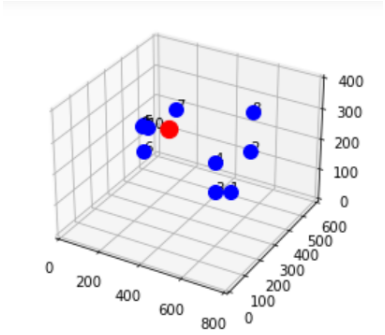

Fig. 7 Run 3: 3D Simulation of SwarmSats and Debris Object

These simulations validate key mission behaviours visually and algorithmically by including swarming, stabilization and coordination. It allows rapid prototyping of control logic, agent role assignment, and capture dynamics. This serves as a precursor to orbital-level simulations, where the same agent control logic could be incorporated into tools like STK or poliastro [18]. Future refinements of this simulation would include orbital elements (semi-major axis, eccentricity, inclination and RAAN), gravitational forces and perturbations, relative motion in orbital frames, thruster-based trajectory control, accurate SwarmSat specifications and real-time capture results with selected debris properties and motion data for more accurate predictions.

B. Theory and Calculations for Mission Considerations

The feasibility of the SwarmSat mission concept relies on several key considerations, including SwarmSat design, capture mechanisms, stabilization strategies, fuel consumption, and external forces. These factors are essential in ensuring the viability of the mission and optimizing energy-efficient operations. Jupyter Notebook was used to calculate the following:

- Orbital access criteria: Inclination, altitude, perigee/apogee matching to optimize rendezvous.
- Fuel consumption modeling: ΔV requirements for agent maneuvers were computed using impulsive thrust equations and mass flow rates for stabilization. This includes calculating fuel consumption for the rendezvous capture and for stabilization.
- Tumbling stabilization: Rotational energy dissipation was estimated using angular momentum exchange principles. This includes the combined angular velocity between the SwarmSat and debris post-capture.
- The performance of net and electromagnetic tethering mechanics was evaluated to minimize residual motion. This includes stress values, elastic deformation, thermal properties and net volume calculations in a CubeSat.

1. SwarmSat Design and Deployment

The SwarmSats are designed based on the RemoveDebris CubeSat mission architecture by the University of Surrey [19]. The proposed agents will have solar panels for optimal power management, and docking mechanisms similar to Branz et al.'s [20] CubeSat docking study to allow refueling or servicing. The mission will deploy multiple CubeSats to conduct distributed capture operations, optimizing for low fuel consumption and operational redundancy. It is crucial to note that the most important mitigation technique lies within the design process of the spacecraft itself. NASA has implemented rules stating spacecraft and upper stages must be designed to eliminate or minimize debris released during normal operations, and, all spacecraft, including this mission concept, must have enough propellant to lower their orbit such that the spacecraft deorbits within 25 years. The following calculations below are based on assumptions, this is reflected in the code provided in Tang's Honours thesis [7].

2. Capture Mechanism: Net Material and Electromagnetic Linkage

The debris capture method uses Ultra-High Molecular Weight Polyethylene (UHMWPE) nets, chosen for their superior ballistic performance over Kevlar [21]. Stress-strain analysis shows UHMWPE has a tensile strength of 20 MPa, ensuring it can withstand dynamic forces. However, further Finite Element Analysis (FEA) is required to evaluate loading conditions, creep deformation, and safety factors.

Additionally, electromagnetic coils are proposed for post-capture debris linkage. Research by NASA [22] suggests oscillating magnetic fields can enhance maneuverability. The heat transfer equation allows for calculation

of the temperature across the system:

$$Q = \frac{k \cdot A \cdot \Delta T}{d} \tag{1}$$

Where, Q is the heat transfer rate (Watts), k is the thermal conductivity of the material (W/m·K), A is the area through which heat is being transferred (m^2), ΔT is the temperature difference across the material (°C) and d is the thickness of the material (m), is used in simulations to evaluate coil heating, ensuring thermal stability within CubeSat operational limits.

3. Forces Exerted by Captured Debris

The forces affecting debris capture include:

Debris Momentum During Capture: Provided that the debris has a relative velocity v m/s to the SwarmSat, and is captured by the net and brought to a stop over time Δt (s), the force due to this can be estimated using Newton's second law [23]:

$$F = \frac{\Delta p}{\Delta t} = \frac{m \cdot v}{\Delta t} \tag{2}$$

where m is the mass of the debris. The actual shape, mass, and rotational inertia of debris objects will significantly influence the required stabilization ΔV and burn time.

Gravitational Forces: Although the debris pieces of interest are classified as small, gravitational attraction between large pieces of debris and the SwarmSat might be non-negligible. This issue must be considered if the SwarmSat encounters a large piece of debris in it's path when trying to retrieve a smaller piece. Additionally, as the debris chains increase in size, the CubeSats will need to consider this effect. Newton's law of universal gravitation [24] must be considered,

$$F = G\frac{m_1 m_2}{r^2} \tag{3}$$

Dynamic Forces: If the SwarmSat with the captured debris undergoes maneuvers, accelerations will introduce dynamic loads. Another way of stating, Newton's second law, $F = m \cdot a$, where a is the acceleration must be considered.

Tumbling Debris: Rotational motion may introduce extra stress. To quantify this, the conservation of angular momentum [25] is used:

$$I_{satellite} \times \omega_{satellite\_before} + I_{debris} \times \omega_{debris\_before} = (I_{satellite} + I_{debris}) \times \omega_{combined\_after} \tag{4}$$

Where $I(kg.m^2)$ is the moment of inertia and ω (rad/s) is the angular velocity.

Using this equation, $\omega_{combined\_after}$ can be found:

$$\omega_{combined\_after} = \frac{I_{satellite} \times \omega_{satellite\_before} + I_{debris} \times \omega_{debris\_before}}{I_{satellite} + I_{debris}} \tag{5}$$

4. Fuel Consumption for Manuever and Stablization

Fuel consumption is calculated using the Tsiolkovsky rocket equation [26]:

$$\Delta V = I_{sp}.g_0.ln(\frac{m_{initial}}{m_{final}}) \tag{6}$$

Where, ΔV is the change in velocity, I_{sp} is the specific impulse of the thruster, g_0 is the standard gravitational acceleration ($9.81 m/s^2$), $m_{initial}$ is the initial mass of the spacecraft before the fuel is burnt and m_{final} is the final mass of the spacecraft after the fuel is burnt.

The estimated temperature rise due to electromagnetic coil activation is 0.23°C, resulting in a combined CubeSat and coil temperature of 80.23°C, which remains within UHMWPE's safe operational range. For comparison, Kevlar exhibits similar thermal safety properties, with a temperature rise of 0.15°C and a combined system temperature of 80.15°C, confirming its viability as an alternative material. The estimated electric field at UHMWPE is $1.00e^{+04}$ V/m, confirming safe resistivity and dielectric strength. UHMWPE operates within safe temperature limits in Low Earth Orbit (LEO), and its volume fits within the allowable limits for a 3U CubeSat.

The combined system (debris + SwarmSat) experiences a post-capture angular velocity of 0.33 rad/s, indicating significant tumbling motion that requires stabilization. The initial transfer maneuver requires 0.0008 kg of fuel,

corresponding to an estimated ΔV of 0.11 m/s. A subsequent maneuver for fine adjustments consumes 0.0002 kg of fuel, demonstrating an efficient fuel expenditure for rendezvous and capture. The stabilization maneuver, required to null out the debris' rotational motion, consumes 0.0135 kg of fuel. The burn time required for stabilization is 330 seconds (5.5 minutes), suggesting a prolonged maneuver to counteract the debris' tumbling motion.
Results from Jupyter Notebook indicate that despite a low ΔV requirement for rendezvous, stabilization is more fuel-intensive, reinforcing the need for energy-efficient thruster design. The current analysis confirms the feasibility of swarm-based ADR using UHMWPE nets, electromagnetic linkage, and thruster-based stabilization. However, further FEA modeling, real-world thermal tests, and optimization algorithms are required to refine the final design. For full technical details, including detailed calculations, Python simulations, STK/TAROT analyses, and additional derivations, readers may request for Tang's Honours thesis [7].

III. Discussion

The results confirm the potential of swarm robotics for ADR, particularly in addressing multiple debris targets within a single mission. The modular nature of CubeSat-based SwarmSats allows scalable deployment with adaptable mission profiles based on debris distribution. The inclusion of multiple capture strategies, such as UHMWPE nets and electromagnetic adhesion, provides redundancy and flexibility, enabling the swarm to handle a variety of debris geometries. However, for successful real-world implementation, additional factors must be further addressed:

- **Material selection and durability:** The SwarmSat components and net material must withstand the harsh conditions of space, including radiation exposure, atomic oxygen, and thermal cycling. Although UHMWPE was verified as feasible through early stress/temperature calculations, future work should incorporate realistic material properties (i.e. exact thickness, net geometry) and subject the design to experimental validation in simulated orbital conditions.
- **Fuel consumption and maneuverability:** While ΔV requirements have been kept low in this study, the SwarmSats' maneuverability, particularly for post-capture stabilization, needs to be further refined. The current simulations assume known transfer windows and idealized propulsion systems. Future work should incorporate system-specific propulsion parameters and assess multi-target chaining missions using optimized trajectory planning (e.g., similar to Cerf et al.'s [6] three-stage optimization framework for high-thrust vehicles).
- **Collision avoidance and autonomy:** Collision avoidance has been implemented in both 2D and 3D simulations. However, real-world implementation requires fully autonomous fault-tolerant agents capable of avoiding other agents and dynamic debris trajectories in a non-cooperative environment. Additional work is needed to build in higher-fidelity swarm intelligence and include more sophisticated navigation based on probabilistic collision models.
- **Target uncertainty and catalog limitations:** Exact debris parameters such as size and mass are often not explicitly defined in available catalogs. Future work must either incorporate estimation techniques or make assumptions more transparent. Additional metrics such as probability-severity (P–S) scoring, derived from kinetic energy and collision likelihood, should be integrated to refine debris prioritization.
- **Time-referenced orbital data:** While orbital proximity between objects was verified via STK and TAROT access reports, absolute position data and epochs were not always referenced explicitly. Future simulations should use Two-Line Element (TLE) derived state vectors with consistent epoch time to validate feasibility of grouping multiple targets within short windows.
- **Mission scalability and cost:** The feasibility of deploying a fleet of SwarmSats for large-scale ADR operations depends on cost-effective manufacturing, launch logistics, and operational longevity. A full mission cost-benefit analysis, including risk and insurance assessments, must be developed to support future implementation.
- **Mission sustainability and obsolescence:** CubeSats have limited operational lifespans, typically ranging from a few months to a few years. This mission concept must ensure agents deorbit safely or can be retrieved once non-functional. To prevent contributing to the debris problem, onboard fault detection, autonomous end-of-life disposal, and compliance with international debris mitigation guidelines should be included in the system design.

Furthermore, future iterations of the existing 2D and 3D simulations in inertial planes will work to incorporate increase orbital fidelity by simulating approach trajectories relative to tumbling debris in orbit, producing path plots that reflect the periodic helical approach behavior expected in real scenarios.

Several simplifications such as uniform agent capabilities, idealized inertial frames, and the use of estimated values for mass, size, and angular momentum have been made in the preliminary feasibility study. These will need refinement in subsequent iterations through more accurate modeling of net geometry, magnetic field strength, drag

modeling, SwarmSat bus design constraints, and real-world environmental interactions.

A systems engineering approach was applied throughout this research to ensure that all mission elements—agent design, software autonomy, orbital access, mechanical capture, and thermal/fuel constraints were holistically evaluated. For further guidance on mission architecture development and support systems, readers are referred to the NASA Systems Engineering Handbook [27].

IV. Conclusion

This research presents a scalable and systematic approach to mitigating the growing challenge of space debris. By enabling autonomous and collaborative swarm behavior, the proposed mission concept demonstrates the feasibility of using CubeSat agents to target, capture, and stabilize hazardous debris in Low Earth Orbit (LEO). Integrated simulations using STK, TAROT, and Python validated key mission elements, including agent coordination, access geometry, and collision avoidance. The modularity of the swarm allows flexible deployment and redundancy through multiple capture mechanisms, such as UHMWPE nets and electromagnetic adhesion. However, further analysis is required in areas such as fuel optimization, material performance under space conditions, autonomous behavior under uncertainty, and mission sustainability and obsolescence. Future work includes refining simulations with TLE-derived orbital models, enhancing realism by incorporating non-inertial dynamics, and extending algorithmic robustness for fault tolerance. This research contributes to the foundational design of autonomous, swarm-based ADR systems and supports global efforts to ensure the long-term safety and sustainability of orbital operations.

Acknowledgments

I wish to express sincere gratitude to the individuals whose support, guidance, and encouragement have contributed significantly to the development and completion of this research.

Alice Bowman *Mission Operations Manager and Group Supervisor at Johns Hopkins University Applied Physics Laboratory*, for overseeing this research. Her expert mentorship in mission operations and systems engineering and her guidance has been instrumental in shaping this study and validating its application to ADR strategies.

Danielle Moreau, *Associate Professor at the University of New South Wales*, for her supervision of my undergraduate Honours thesis, which laid the foundation for this extended research.

Sorina Lupu, *Researcher at the California Institute of Technology (Caltech)*, whose insightful suggestions for future work were directly incorporated into this paper. Her contributions have significantly enriched the technical depth and direction of the study.

Jackie Carpenter, *Founder and Director of One Giant Leap Australia*, for her practical advice and encouragement in preparing for the SpaceOps 2025 conference, and for supporting my participation in international research engagement.

Dianea Phillips, *CEO and Aerospace Educator of Science Yourself!*, for her kind hospitality and generosity in hosting me during my stay in Canada for the conference.

John Best, *Chief Technology Officer at Thales Australia*, for his support in forwarding this work to subject matter experts for review, and for ensuring the paper was cleared for publication from a Thales perspective.

Michael Clark, *Adjunct Professor at Western Sydney University and former Director of Technical Strategy at Thales Australia*, for his valuable feedback, questions, and critique that helped strengthen the technical scope and clarity of the paper.

Michael Evans, *Head of Safety Engineering and ILS Disciplines at Thales, Above Water Systems, Australia* for his helpful comment and proofreading support.

Pinak Sharma, *Space Mission Design Engineer at Saber Astronautics*, for reviewing the paper to ensure it was well-structured and presentable for publication, and for posing key questions that enhanced the clarity and completeness of the work.

Finally, I extend heartfelt thanks to my family and friends for their unwavering support, patience, and encouragement, which have been a constant source of motivation throughout this journey. And of course, special thanks to my adorable border collie, Toffee, for bringing joy into my life.

Appendix

A. Required Velocity for SwarmSats

The difference in inclination is:

$$\Delta i = 98^\circ 69' - 98^\circ 68' = 1' \tag{7}$$

Plane change at apogee:

$$\Delta v_{plane} = 2V_i \sin(\frac{\Delta i}{2}) \tag{8}$$

Substituting the values provided:

$$\Delta v_{plane} = 2(7.6\text{km/s}) \sin(0.5) \tag{9}$$

$$\Delta v_{plane} \approx 0.133\text{km/s} \tag{10}$$

Given the two debris cases of CZ-6A (NORAD CAT ID: 54974) Apogee: 842 km, Perigee: 677 km. The semi-major axis: r_1 is,

$$r_1 = \frac{842 + 677}{2} + 6371\text{km} = 7130.5\text{km} \tag{11}$$

and CZ-6A (NORAD CAT ID: 56629) Apogee: 842 km, Perigee: 690 km. The semi-major axis: r_2 is ,

$$r_2 = \frac{842 + 690}{2} + 6371\text{km} = 7137\text{km} \tag{12}$$

These values can then be substituted to find the altitude change (Hohmann transfer approximation):

$$\Delta v_1 = \sqrt{\frac{\mu}{r_1}}(\sqrt{\frac{2r_2}{r_1 + r_2}} - 1) \tag{13}$$

$$\Delta v_2 = \sqrt{\frac{\mu}{r_2}}(1 - \sqrt{\frac{2r_2}{r_1 + r_2}}) \tag{14}$$

Where μ is the Earth's gravitational parameter $3.986 \times 10^{14} m^3/s^2$ and r_1 is the initial orbit's semi major axis and r_2 is the final orbit's semi major axis. Given the major difference in altitudes, v will be significantly large.

Substituting the calculated values, it is found that: $\Delta v_1 \approx 3.41$m/s and $\Delta v_2 \approx 3.41$m/s.

Eccentricity is given by:

$$e = \frac{r_{\text{apogee}} - r_{\text{perigee}}}{r_{\text{apogee}} + r_{\text{perigee}}} \tag{15}$$

Substituting the values provided, CZ-6A (NORAD CAT ID: 54974) eccentricity is $e_1 \approx 0.109$ and CZ-6A (NORAD CAT ID: 56629) eccentricity is $e_2 \approx 0.099$.

Using Kepler's Third Law, the orbital period can be found:

$$T^2 = \frac{4\pi^2 r^3}{GM} \tag{16}$$

where T is the orbital period, G is the gravitational constant and M is the mass of the earth. Substituting the given values,

$${T_1}^2 = \frac{4\pi^2 (7150.5 \times 10^3)^3}{(6.6743 \times 10^{-11})(5.972 \times 10^{24})} \tag{17}$$

$$T_1 = 6017.58s \approx 100.3\text{mins} \tag{18}$$

$${T_2}^2 = \frac{4\pi^2 (7137 \times 10^3)^3}{(6.6743 \times 10^{-11})(5.972 \times 10^{24})} \tag{19}$$

$$T_2 = 6000.54s \approx 100.0\text{mins} \tag{20}$$

B. Run 2: Simulation Data of SwarmSats in Planar Space

Debris is tumbling at position (549.81, 305.00) Debris is tumbling at position (549.25, 309.98) Debris is tumbling at position (548.32, 314.94) Debris is tumbling at position (547.01, 319.87) Debris is tumbling at position (545.34, 324.74) Debris is tumbling at position (543.30, 329.55) Debris is tumbling at position (540.91, 334.29) Debris is tumbling at position (538.16, 338.94) Debris is tumbling at position (535.07, 343.50) Debris is tumbling at position (531.64, 347.94) Debris is tumbling at position (527.88, 352.27) Debris is tumbling at position (523.80, 356.46) Debris is tumbling at position (519.41, 360.52) Debris is tumbling at position (514.73, 364.42) Agent 3 is near the debris at (514.73, 364.42) Debris is tumbling at position (509.75, 368.16) Agent 3 is near the debris at (509.75, 368.16) Debris is tumbling at position (504.51, 371.74) Agent 3 is near the debris at (504.51, 371.74) Debris is tumbling at position (499.00, 375.13) Agent 3 is near the debris at (499.00, 375.13) Debris is tumbling at position (493.24, 378.33) Agent 3 is near the debris at (493.24, 378.33) Debris is tumbling at position (487.25, 381.34) Agent 3 is near the debris at (487.25, 381.34) Agent 5 is near the debris at (487.25, 381.34) Debris is tumbling at position (481.05, 384.15) Agent 3 is near the debris at (481.05, 384.15) Agent 5 is near the debris at (481.05, 384.15) Debris is tumbling at position (474.64, 386.74) Agent 3 is near the debris at (474.64, 386.74) Agent 5 is near the debris at (474.64, 386.74) Debris is tumbling at position (468.04, 389.12) Agent 3 is near the debris at (468.04, 389.12) Agent 5 is near the debris at (468.04, 389.12) Agent 8 is near the debris at (468.04, 389.12) Debris is tumbling at position (461.27, 391.28) Agent 3 is near the debris at (461.27, 391.28) Agent 5 is near the debris at (461.27, 391.28) Agent 8 is near the debris at (461.27, 391.28) Debris is tumbling at position (454.35, 393.20) Agent 3 is near the debris at (454.35, 393.20) Agent 5 is near the debris at (454.35, 393.20) Agent 8 is near the debris at (454.35, 393.20) Agent 9 is near the debris at (454.35, 393.20) Debris is tumbling at position (447.30, 394.90) Agent 3 is near the debris at (447.30, 394.90) Agent 5 is near the debris at (447.30, 394.90) Agent 5 captured the debris at (447.30, 394.90) Agent 5 is stabilizing the debris at (447.30, 394.90) Agent 8 is stabilizing the debris at (447.30, 394.90) Agent 9 is stabilizing the debris at (447.30, 394.90) Debris captured and stabilized! Total time: 1.34 seconds Agents involved in stabilization: [5, 8, 9]

C. Run 1: Simulation Data of SwarmSats ad Debris Object

Debris is tumbling at position (226.31, 387.45, 222.15) Agent 7 is near the debris at (226.31, 387.45, 222.15) Debris is tumbling at position (228.30, 387.65, 222.34) Agent 7 is near the debris at (228.30, 387.65, 222.34) Debris is tumbling at position (230.28, 387.95, 222.64) Agent 7 is near the debris at (230.28, 387.95, 222.64) Debris is tumbling at position (232.24, 388.34, 223.04) Agent 7 is near the debris at (232.24, 388.34, 223.04) Debris is tumbling at position (234.18, 388.84, 223.54) Agent 7 is near the debris at (234.18, 388.84, 223.54) Debris is tumbling at position (236.09, 389.43, 224.13) Agent 7 is near the debris at (236.09, 389.43, 224.13) Debris is tumbling at position (237.97, 390.11, 224.81) Agent 7 is near the debris at (237.97, 390.11, 224.81) Debris is tumbling at position (239.81, 390.89, 225.59) Agent 7 is near the debris at (239.81, 390.89, 225.59) Debris is tumbling at position (241.61, 391.76, 226.46) Agent 7 is near the debris at (241.61, 391.76, 226.46) Debris is tumbling at position (243.36, 392.72, 227.42) Agent 7 is near the debris at (243.36, 392.72, 227.42) Debris is tumbling at position (245.07, 393.77, 228.47) Agent 7 is near the debris at (245.07, 393.77, 228.47) Agent 7 captured the debris at (245.07, 393.77, 228.47) Agent 7 is stabilizing the debris at (245.07, 393.77, 228.47) Agent 6 is stabilizing the debris at (245.07, 393.77, 228.47) Agent 5 is stabilizing the debris at (245.07, 393.77, 228.47) Debris captured and stabilized! Total time: 5.07 seconds Agents involved in stabilization: [7, 6, 5]

D. Run 2: Simulation Data of SwarmSats ad Debris Object

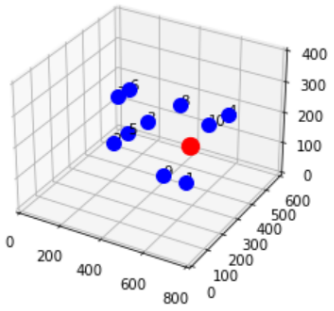

Fig. 8 Run 2: 3D Simulation of SwarmSats and Debris Object

Debris is tumbling at position (593.24, 286.65, 195.73) Agent 10 is near the debris at (593.24, 286.65, 195.73) Debris is tumbling at position (595.23, 286.85, 195.93) Agent 10 is near the debris at (595.23, 286.85, 195.93) Debris is tumbling at position (597.21, 287.15, 196.23) Agent 10 is near the debris at (597.21, 287.15, 196.23) Debris is tumbling at position (599.17, 287.55, 196.62) Agent 10 is near the debris at (599.17, 287.55, 196.62) Debris is tumbling at position (601.11, 288.04, 197.12) Agent 10 is near the debris at (601.11, 288.04, 197.12) Debris is tumbling at position (603.02, 288.63, 197.71) Agent 10 is near the debris at (603.02, 288.63, 197.71) Debris is tumbling at position (604.90, 289.32, 198.39) Agent 10 is near the debris at (604.90, 289.32, 198.39) Debris is tumbling at position (606.74, 290.10, 199.17) Agent 10 is near the debris at (606.74, 290.10, 199.17) Debris is tumbling at position (608.54, 290.97, 200.04) Agent 10 is near the debris at (608.54, 290.97, 200.04) Debris is tumbling at position (610.30, 291.93, 201.00) Agent 10 is near the debris at (610.30, 291.93, 201.00) Debris is tumbling at position (612.00, 292.97, 202.05) Agent 10 is near the debris at (612.00, 292.97, 202.05) Debris is tumbling at position (613.65, 294.10, 203.18) Agent 10 is near the debris at (613.65, 294.10, 203.18) Debris is tumbling at position (615.25, 295.31, 204.39) Agent 10 is near the debris at (615.25, 295.31, 204.39) Debris is tumbling at position (616.78, 296.60, 205.68) Agent 10 is near the debris at (616.78, 296.60, 205.68) Debris is tumbling at position (618.24, 297.96, 207.04) Agent 10 is near the debris at (618.24, 297.96, 207.04) Debris is tumbling at position (619.63, 299.40, 208.47) Agent 10 is near the debris at (619.63, 299.40, 208.47) Debris is tumbling at position (620.95, 300.90, 209.98) Agent 10 is near the debris at (620.95, 300.90, 209.98) Agent 10 captured the debris at (620.95, 300.90, 209.98) Agent 10 is stabilizing the debris at (620.95, 300.90, 209.98) Agent 1 is stabilizing the debris at (620.95, 300.90, 209.98) Agent 4 is stabilizing the debris at (620.95, 300.90, 209.98) Debris captured and stabilized! Total time: 4.96 seconds Agents involved in stabilization: [10, 1, 4]

E. Run 3: Simulation Data of SwarmSats ad Debris Object

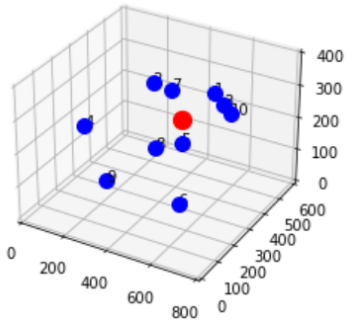

Fig. 9 Run 3: 3D Simulation of SwarmSats and Debris Object

Debris is tumbling at position (443.71, 375.59, 226.00) Agent 7 is near the debris at (443.71, 375.59, 226.00) Debris is tumbling at position (445.70, 375.79, 226.20) Agent 7 is near the debris at (445.70, 375.79, 226.20) Debris is tumbling at position (447.67, 376.09, 226.50) Agent 7 is near the debris at (447.67, 376.09, 226.50) Debris is tumbling at position (449.63, 376.49, 226.89) Agent 7 is near the debris at (449.63, 376.49, 226.89) Debris is tumbling at position (451.57, 376.98, 227.39) Agent 7 is near the debris at (451.57, 376.98, 227.39) Debris is tumbling at position (453.48, 377.57, 227.98) Agent 7 is near the debris at (453.48, 377.57, 227.98) Debris is tumbling at position (455.36, 378.26, 228.67) Agent 7 is near the debris at (455.36, 378.26, 228.67) Debris is tumbling at position (457.20, 379.04, 229.44) Agent 7 is near the debris at (457.20, 379.04, 229.44) Debris is tumbling at position (459.00, 379.91, 230.31) Agent 7 is near the debris at (459.00, 379.91, 230.31) Debris is tumbling at position (460.76, 380.87, 231.27) Agent 7 is near the debris at (460.76, 380.87, 231.27) Debris is tumbling at position (462.46, 381.91, 232.32) Agent 7 is near the debris at (462.46, 381.91, 232.32) Debris is tumbling at position (464.11, 383.04, 233.45) Agent 7 is near the debris at (464.11, 383.04, 233.45) Debris is tumbling at position (465.71, 384.25, 234.66) Agent 7 is near the debris at (465.71, 384.25, 234.66) Debris is tumbling at position (467.24, 385.54, 235.95) Agent 7 is near the debris at (467.24, 385.54, 235.95) Debris is tumbling at position (468.70, 386.90, 237.31) Agent 7 is near the debris at (468.70, 386.90, 237.31) Debris is tumbling at position (470.09, 388.34, 238.74) Agent 7 is near the debris at (470.09, 388.34, 238.74) Debris is tumbling at position (471.41, 389.84, 240.25) Agent 7 is near the debris at (471.41, 389.84, 240.25) Debris is tumbling at position (472.66, 391.41, 241.81) Agent 7 is near the debris at (472.66, 391.41, 241.81) Debris is tumbling at position (473.82, 393.03, 243.44) Agent 1 is near the debris at (473.82, 393.03, 243.44) Agent 7 is near the debris at (473.82, 393.03, 243.44) Debris is tumbling at position (474.90, 394.72, 245.12) Agent

1 is near the debris at (474.90, 394.72, 245.12) Agent 7 is near the debris at (474.90, 394.72, 245.12) Debris is tumbling at position (475.90, 396.45, 246.86) Agent 1 is near the debris at (475.90, 396.45, 246.86) Agent 7 is near the debris at (475.90, 396.45, 246.86) Debris is tumbling at position (476.80, 398.23, 248.64) Agent 1 is near the debris at (476.80, 398.23, 248.64) Agent 7 is near the debris at (476.80, 398.23, 248.64) Debris is tumbling at position (477.62, 400.06, 250.47) Agent 1 is near the debris at (477.62, 400.06, 250.47) Agent 7 is near the debris at (477.62, 400.06, 250.47) Debris is tumbling at position (478.34, 401.92, 252.33) Agent 1 is near the debris at (478.34, 401.92, 252.33) Agent 7 is near the debris at (478.34, 401.92, 252.33) Debris is tumbling at position (478.98, 403.82, 254.23) Agent 1 is near the debris at (478.98, 403.82, 254.23) Agent 7 is near the debris at (478.98, 403.82, 254.23) Debris is tumbling at position (479.51, 405.75, 256.16) Agent 1 is near the debris at (479.51, 405.75, 256.16) Agent 7 is near the debris at (479.51, 405.75, 256.16) Debris is tumbling at position (479.95, 407.70, 258.11) Agent 1 is near the debris at (479.95, 407.70, 258.11) Agent 7 is near the debris at (479.95, 407.70, 258.11) Debris is tumbling at position (480.29, 409.67, 260.08) Agent 1 is near the debris at (480.29, 409.67, 260.08) Agent 7 is near the debris at (480.29, 409.67, 260.08) Debris is tumbling at position (480.53, 411.66, 262.06) Agent 1 is near the debris at (480.53, 411.66, 262.06) Agent 7 is near the debris at (480.53, 411.66, 262.06) Debris is tumbling at position (480.67, 413.65, 264.06) Agent 1 is near the debris at (480.67, 413.65, 264.06) Agent 7 is near the debris at (480.67, 413.65, 264.06) Debris is tumbling at position (480.71, 415.65, 266.06) Agent 1 is near the debris at (480.71, 415.65, 266.06) Agent 7 is near the debris at (480.71, 415.65, 266.06) Debris is tumbling at position (480.65, 417.65, 268.06) Agent 1 is near the debris at (480.65, 417.65, 268.06) Agent 7 is near the debris at (480.65, 417.65, 268.06) Debris is tumbling at position (480.50, 419.64, 270.05) Agent 1 is near the debris at (480.50, 419.64, 270.05) Agent 7 is near the debris at (480.50, 419.64, 270.05) Debris is tumbling at position (480.24, 421.63, 272.03) Agent 1 is near the debris at (480.24, 421.63, 272.03) Agent 7 is near the debris at (480.24, 421.63, 272.03) Debris is tumbling at position (479.88, 423.59, 274.00) Agent 1 is near the debris at (479.88, 423.59, 274.00) Agent 7 is near the debris at (479.88, 423.59, 274.00) Debris is tumbling at position (479.43, 425.54, 275.95) Agent 1 is near the debris at (479.43, 425.54, 275.95) Agent 7 is near the debris at (479.43, 425.54, 275.95) Debris is tumbling at position (478.88, 427.47, 277.87) Agent 1 is near the debris at (478.88, 427.47, 277.87) Agent 7 is near the debris at (478.88, 427.47, 277.87) Debris is tumbling at position (478.23, 429.36, 279.77) Agent 1 is near the debris at (478.23, 429.36, 279.77) Agent 7 is near the debris at (478.23, 429.36, 279.77) Debris is tumbling at position (477.49, 431.22, 281.62) Agent 1 is near the debris at (477.49, 431.22, 281.62) Agent 7 is near the debris at (477.49, 431.22, 281.62) Debris is tumbling at position (476.66, 433.03, 283.44) Agent 1 is near the debris at (476.66, 433.03, 283.44) Agent 7 is near the debris at (476.66, 433.03, 283.44) Debris is tumbling at position (475.73, 434.81, 285.22) Agent 1 is near the debris at (475.73, 434.81, 285.22) Agent 7 is near the debris at (475.73, 434.81, 285.22) Debris is tumbling at position (474.72, 436.54, 286.94) Agent 1 is near the debris at (474.72, 436.54, 286.94) Agent 7 is near the debris at (474.72, 436.54, 286.94) Debris is tumbling at position (473.63, 438.21, 288.62) Agent 1 is near the debris at (473.63, 438.21, 288.62) Agent 7 is near the debris at (473.63, 438.21, 288.62) Debris is tumbling at position (472.45, 439.83, 290.23) Agent 1 is near the debris at (472.45, 439.83, 290.23) Agent 7 is near the debris at (472.45, 439.83, 290.23) Debris is tumbling at position (471.20, 441.38, 291.79) Agent 1 is near the debris at (471.20, 441.38, 291.79) Agent 7 is near the debris at (471.20, 441.38, 291.79) Debris is tumbling at position (469.86, 442.87, 293.28) Agent 1 is near the debris at (469.86, 442.87, 293.28) Agent 7 is near the debris at (469.86, 442.87, 293.28) Debris is tumbling at position (468.46, 444.30, 294.70) Agent 1 is near the debris at (468.46, 444.30, 294.70) Agent 7 is near the debris at (468.46, 444.30, 294.70) Debris is tumbling at position (466.98, 445.65, 296.06) Agent 1 is near the debris at (466.98, 445.65, 296.06) Agent 7 is near the debris at (466.98, 445.65, 296.06) Debris is tumbling at position (465.44, 446.92, 297.33) Agent 1 is near the debris at (465.44, 446.92, 297.33) Agent 7 is near the debris at (465.44, 446.92, 297.33) Debris is tumbling at position (463.84, 448.12, 298.53) Agent 1 is near the debris at (463.84, 448.12, 298.53) Agent 7 is near the debris at (463.84, 448.12, 298.53) Debris is tumbling at position (462.18, 449.24, 299.64) Agent 1 is near the debris at (462.18, 449.24, 299.64) Agent 7 is near the debris at (462.18, 449.24, 299.64) Debris is tumbling at position (460.47, 450.27, 300.67) Agent 1 is near the debris at (460.47, 450.27, 300.67) Agent 7 is near the debris at (460.47, 450.27, 300.67) Debris is tumbling at position (458.70, 451.21, 301.62) Agent 1 is near the debris at (458.70, 451.21, 301.62) Agent 7 is near the debris at (458.70, 451.21, 301.62) Debris is tumbling at position (456.90, 452.07, 302.47) Agent 1 is near the debris at (456.90, 452.07, 302.47) Agent 7 is near the debris at (456.90, 452.07, 302.47) Debris is tumbling at position (455.05, 452.83, 303.24) Agent 1 is near the debris at (455.05, 452.83, 303.24) Agent 7 is near the debris at (455.05, 452.83, 303.24) Debris is tumbling at position (453.16, 453.50, 303.91) Agent 1 is near the debris at (453.16, 453.50, 303.91) Agent 7 is near the debris at (453.16, 453.50, 303.91) Debris is tumbling at position (451.25, 454.07, 304.48) Agent 1 is near the debris at (451.25, 454.07, 304.48) Agent 7 is near the debris at (451.25, 454.07, 304.48) Debris is tumbling at position (449.31, 454.55, 304.96) Agent 1 is near the debris at (449.31, 454.55, 304.96) Agent 7 is near the debris at (449.31, 454.55, 304.96) Debris is tumbling at position (447.34, 454.93, 305.34) Agent 1 is near the debris at (447.34, 454.93, 305.34) Agent 7 is near the debris at (447.34, 454.93, 305.34) Debris is tumbling at position

(445.36, 455.22, 305.62) Agent 1 is near the debris at (445.36, 455.22, 305.62) Agent 7 is near the debris at (445.36, 455.22, 305.62) Debris is tumbling at position (443.37, 455.40, 305.81) Agent 1 is near the debris at (443.37, 455.40, 305.81) Agent 7 is near the debris at (443.37, 455.40, 305.81) Debris is tumbling at position (441.37, 455.48, 305.89) Agent 1 is near the debris at (441.37, 455.48, 305.89) Agent 7 is near the debris at (441.37, 455.48, 305.89) Debris is tumbling at position (439.37, 455.46, 305.87) Agent 1 is near the debris at (439.37, 455.46, 305.87) Agent 7 is near the debris at (439.37, 455.46, 305.87) Debris is tumbling at position (437.38, 455.35, 305.76) Agent 1 is near the debris at (437.38, 455.35, 305.76) Agent 7 is near the debris at (437.38, 455.35, 305.76) Debris is tumbling at position (435.39, 455.13, 305.54) Agent 1 is near the debris at (435.39, 455.13, 305.54) Agent 7 is near the debris at (435.39, 455.13, 305.54) Debris is tumbling at position (433.41, 454.82, 305.22) Agent 1 is near the debris at (433.41, 454.82, 305.22) Agent 7 is near the debris at (433.41, 454.82, 305.22) Debris is tumbling at position (431.46, 454.40, 304.81) Agent 1 is near the debris at (431.46, 454.40, 304.81) Agent 7 is near the debris at (431.46, 454.40, 304.81) Debris is tumbling at position (429.52, 453.89, 304.30) Agent 1 is near the debris at (429.52, 453.89, 304.30) Agent 7 is near the debris at (429.52, 453.89, 304.30) Debris is tumbling at position (427.62, 453.28, 303.69) Agent 1 is near the debris at (427.62, 453.28, 303.69) Agent 7 is near the debris at (427.62, 453.28, 303.69) Debris is tumbling at position (425.74, 452.58, 302.99) Agent 1 is near the debris at (425.74, 452.58, 302.99) Agent 7 is near the debris at (425.74, 452.58, 302.99) Debris is tumbling at position (423.91, 451.79, 302.20) Agent 1 is near the debris at (423.91, 451.79, 302.20) Agent 7 is near the debris at (423.91, 451.79, 302.20) Debris is tumbling at position (422.11, 450.90, 301.31) Agent 1 is near the debris at (422.11, 450.90, 301.31) Agent 7 is near the debris at (422.11, 450.90, 301.31) Agent 7 captured the debris at (422.11, 450.90, 301.31) Agent 7 is stabilizing the debris at (422.11, 450.90, 301.31) Agent 1 is stabilizing the debris at (422.11, 450.90, 301.31) Agent 2 is stabilizing the debris at (422.11, 450.90, 301.31) Debris captured and stabilized! Total time: 6.95 seconds Agents involved in stabilization: [7, 1, 2]

References

[1] Ansys, "Systems Tools Kit," , n.d.

[2] SaberAstronautics, "TAORT," https://tarot.saberastro.com/, n.d. Software.

[3] MIRAGE, "Space Junk: The Problem Growing Above Us," https://www.miragenews.com/space-junk-the-problem-growing-above-us-1019777/, 2023. Accessed 20-07-2023.

[4] European Space Agency, "Impact chip on ISS Cupola window caused by space debris," , 2016. URL https://www.esa.int/ESA_Multimedia/Images/2016/05/Impact_chip, accessed: March 30, 2025.

[5] ESA, "The current state of space debris," https://www.esa.int/SpaceSafety/SpaceDebris/Thecurrentstateofspacedebris., 2023. Accessed 29-07-2023.

[6] Cerf, M., "Multiple Space Debris Collecting Mission: Optimal Mission Planning." *J Optim Theory Appl*, Vol. 167, 2015, pp. 195–218.

[7] Tang, W., "Multi-Agent Systems for Space Debris Aggregation and Removal: A Technical Feasibility Study," *Undergraduate Research Thesis*, 2023, pp. 42–43.

[8] ESA, "RemoveDebris Mission," *Satellite Missions Catalogue*, 2015.

[9] of Inspector General, N. O., "NASA'S EFFORTS TO MITIGATE THE RISKS POSED BY ORBITAL DEBRIS," , 2021.

[10] Peterson, and E., G., "Target identification and delta-V sizing for active debris removal and improved tracking campaigns," *Proceedings of the 23rd International Symposium on Spaceflight Dynamics*, 2012, pp. 257–268.

[11] Colvin, T. J., Karcz, J., and Wusk, G., "Cost and Benefit Analysis of Orbital Debris Remediation," , 2023.

[12] Gregersen, E., "Space Debris," https://www.britannica.com/technology/space-debris, 2023. Accessed 20-08-2023.

[13] of Defense, U. D., "Satellite Catalog," https://www.space-track.org/#catalog, 2023.

[14] Wertz, J. R., and Larson, W. J., *Space Mission Analysis and Design*, Microcosm Press and Springer, 1999.

[15] Curtis, H. D., *Orbital Mechanics for Engineering Students*, Butterworth-Heinemann, 2010.

[16] NanoAvionics, "CubeSat Propulsion System EPSS," https://nanoavionics.com/cubesat-components/cubesat-propulsion-system-epss/, 2023. Accessed 21-12-2023.

[17] Simone, D., Andreades, M. E. ., Hilmi, C. ., Meo, M. ., Ciampa, M. ., and Francesco, "Proof of concept for a smart composite orbital debris detector," *Acta Astronautica*, Vol. 160, 2019, pp. 499–508.

[18] Python, "poliastro," hhttps://docs.poliastro.space/en/stable/, n.d. Software.

[19] of Surrey, U., "RemoveDebris," https://www.surrey.ac.uk/surrey-space-centre/missions/removedebris, n.d. Accessed 20-08-2023.

[20] Branz, F., Olivieri, L., Sansone, F., and Francesconi, A., "Miniature docking mechanism for CubeSats," *Acta Astronautica*, Vol. 176, 2020, pp. 510–519.

[21] Cha, J.-H., Kim, Y., Kumar, S. K. S., Choi, C., and Kim, C.-G., "Ultra-high-molecular-weight polyethylene as a hypervelocity impact shielding material for space structures," *Acta Astronautica*, Vol. 168, 2020, pp. 182–190.

[22] NASA, "Electromagnets Offer Tantalizing Options for Satellites," https://www.nasa.gov/centers-and-facilities/kennedy/electromagnets-offer-tantalizing-options-for-satellites/, n.d. Accessed 20-08-2023.

[23] Britannica, E., "Newton's second law: F = ma," https://www.britannica.com/science/Newtons-laws-of-motion/Newtons-second-law-F-ma, n.d. Accessed 21-08-2023.

[24] LibreTexts, P., "5.5: Newton's Law of Universal Gravitation," https://phys.libretexts.org/Bookshelves/University_Physics/Physics_(Boundless)/5%3A_Uniform_Circular_Motion_and_Gravitation/5.5%3A_Newtons_Law_of_Universal_Gravitation#:~:text=Newton's%20law%20of%20universal%20gravitation%20states%20that%20every%20point%20mass,of%20the%20distance%20between%20them., n.d.. Accessed 21-08-2023.

[25] LibreTexts, P., "9.6: Conservation of Angular Momentum," https://phys.libretexts.org/Bookshelves/University_Physics/Physics_(Boundless)/9%3A_Rotational_Kinematics_Angular_Momentum_and_Energy/9.6%3A_Conservation_of_Angular_Momentum#:~:text=Just%20as%20linear%20momentum%20is,%E2%86%92Ldt%3D0., n.d.. Accessed 21-08-2023.

[26] of Central Florida, U., "9.7 Rocket Propulsion," https://pressbooks.online.ucf.edu/osuniversityphysics/chapter/9-7-rocket-propulsion/, 2016. Accessed 21-08-2023.

[27] NASA, "NASA Systems Engineering Handbook," , 2007. URL "https://www.nasa.gov/wp-content/uploads/2018/09/nasa_systems_engineering_handbook_0.pdf".